

Polymer Characterization by Thermal Field Flow Fractionation with a Continuous Viscosity Detector

J. J. KIRKLAND, S. W. REMENTER, and W. W. YAU,
*E. I. DuPont de Nemours and Company, Central Research and
Development Department, Experimental Station, P.O. Box 80228,
Wilmington, Delaware 19880-0228*

Synopsis

A sensitive flow viscometer detector has been successfully used with time-delay, exponential-decay thermal field flow fractionation (TDE-TFFF) to produce unique information on polymers. TFFF with a concentration-dependent detector (e.g., refractometer) and a differential capillary viscometer is unable to produce a universal calibration plot that eliminates the necessity of polymer standards for accurate molecular-weight calibration. However, this system directly provides valuable information on the inherent (or intrinsic) viscosity distribution of polymers. Absolute intrinsic viscosity values are measured by TFFF without the need of calibration. Detailed TFFF/inherent-viscosity distribution profiles uniquely describe individual sample differences and are not affected by the experimental conditions used in TFFF separations. These viscosity distributions should be very useful in polymer characterization, since they are closely correlated with polymer end-use and solution properties, as well as to polymer molecule weight.

INTRODUCTION

Thermal field flow fractionation (TFFF) is a promising new separation method for characterizing polymers.¹⁻⁸ Separations are carried out in a thin, open channel formed between two parallel highly polished plates.^{9,10} A temperature gradient across the flow channel is established by maintaining top and bottom plates at different temperatures. As a result of this temperature difference, sample components are pushed against one wall. Higher molecular weight (MW) components that are closer to this wall are intercepted by slow-moving flowstreams of the essentially laminar flow profile developed between the thin gap between the parallel plates. These high MW materials lag behind and elute after lower MW solutes that are intercepted by faster flowstreams away from the channel wall.

Compared to size-exclusion chromatography (SEC), TFFF gives better resolution for higher molecular weight accuracy and superior capability for characterizing ultrahigh molecular-weight (MW) polymer samples. At present, quantitative polymer molecular weight determination by TFFF or SEC requires calibration with standards of known MW standards. However, absolute MW calibration is not always possible, because proper MW standards are often not available for direct calibration.

Polymers typically are characterized by molecular weight values. However, intrinsic viscosity ($[\eta]$) also has long been recognized as a very useful polymer

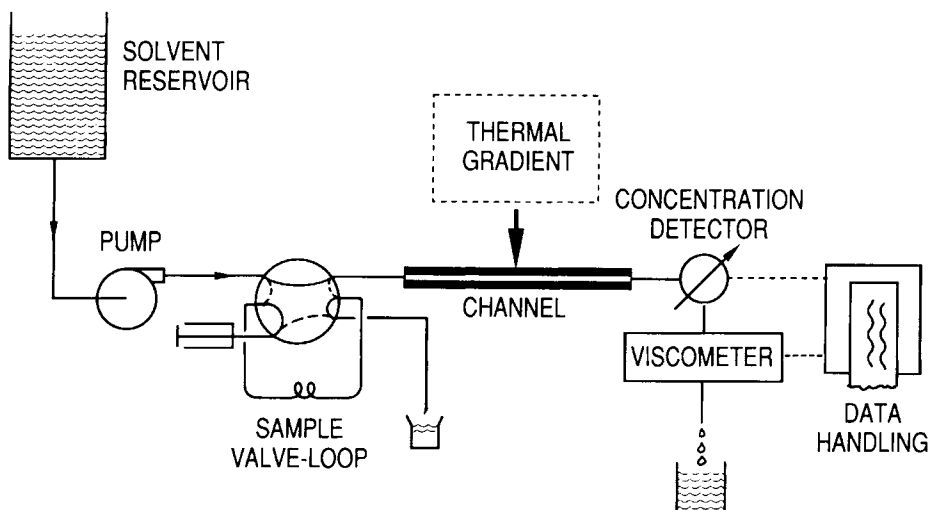


Fig. 1. Schematic of a thermal field flow fractionation apparatus with an online viscometer detector.

characterization parameter. Polymer end-use and solution properties often may be correlated as well by polymer intrinsic viscosity values as by polymer MW.

With the addition of a sensitive online viscometer, TFFF can provide a complete intrinsic viscosity characterization of a polymer sample.^{11,12} Absolute polymer $[\eta]$ values are measured at every TFFF elution volume without the need of calibration. Detailed features of TFFF- $[\eta]$ distribution profiles are unique to individual sample differences and not affected by differences in specific TFFF experimental conditions. In this paper, two common polymer-solvent systems are studied to demonstrate the advantages and limitations of using an on-line viscometer with TFFF.

THEORY

The TFFF effluent is continuously monitored by a concentration detector (e.g., a differential refractometer) and a differential pressure capillary viscometer connected in series. A TFFF apparatus with a sensitive flow viscometer detector is shown in Figure 1. Under the influence of the applied temperature gradient across the TFFF channel, polymer molecules of different molecular weight (MW) and intrinsic viscosity ($[\eta]$) are separated in the TFFF channel and elute at different times. For broad molecular-weight distribution (MWD) polymers, two different-shaped TFFF elution profiles are detected: one by the differential refractometer and one by the viscometer. The relative peak heights of these two TFFF elution profiles provide the means for calculating the intrinsic viscosity of the polymer and the sample polydispersity.

Polymer intrinsic viscosity $[\eta]$ is related to polymer molecular weight (M) through the Mark-Houwink equation:

$$[\eta] = KM^a \quad (1)$$

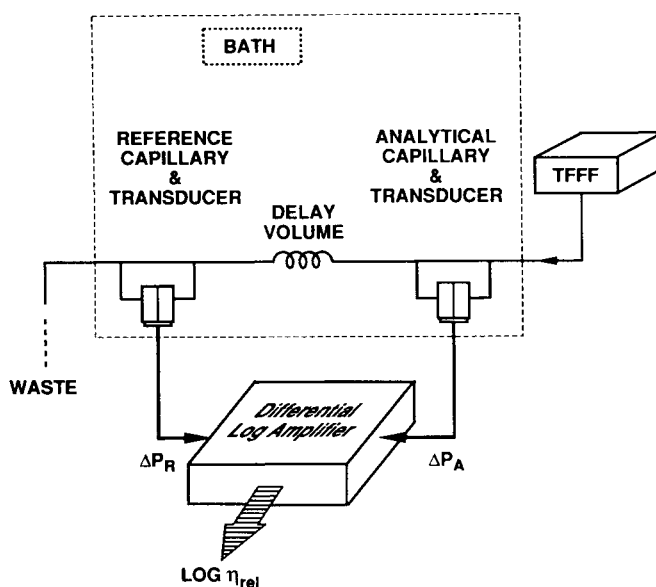


Fig. 2. Viscometer detector configuration for TFFF apparatus.

where K and a are Mark-Houwink viscosity constants. The usual value for a falls between 0.5 and 0.8 for random-coil polymers. Intrinsic viscosity is, therefore, a fundamental polymer characterization parameter that provides both size and MW information for polymers.

Polymer concentrations inherent in TFFF effluents normally are quite dilute because of band-broadening processes occurring during the separation. This feature of low sample concentration has two practical implications in the continuous viscosity detection. First, the very low concentration permits a direct $[\eta]$ measurement during TFFF separations; single-point $[\eta]$ values can be determined by using

$$\text{inherent viscosity: } \eta_{\text{inh}} = (\ln \eta_{\text{rel}})/C \quad (2a)$$

$$\text{intrinsic viscosity: } [\eta] = \lim_{C \rightarrow 0} \eta_{\text{inh}} = \lim_{C \rightarrow 0} \eta_{\text{rel}} \quad (2b)$$

without the need for sample concentration extrapolation normally required for most inherent viscosity determination. Second, the low sample concentration in TFFF effluents demands extraordinary sensitivity of the viscometer to detect small viscosity differences. The viscometer shown in Figure 1 is designed to optimize detection sensitivity by using a logarithmic referencing scheme to compensate for system flow rate and temperature fluctuations.¹³

The viscometer used in this study consists of two sets of capillary and pressure transducer assemblies connected in series, as shown in Figure 2. Liquid flows through the analytical and the reference capillary continuously; flow does not pass through the pressure transducers. A delay volume is placed between the analytical and the reference capillary. The purpose of this delay

volume is to ensure that no sample reaches the reference capillary during the time that the sample viscosity is monitored in the analytical capillary. The differential-pressure signals from the analytical capillary ΔP_A and the reference capillary ΔP_R are fed to a differential logarithmic amplifier. By using a delay volume, the sample ΔP_A signal is always accurately referenced against the solvent ΔP_R signal in the differential logarithmic amplifier. The output S of the log amplifier gives the desired measure of the logarithm of the sample relative viscosity $\ln \eta_{\text{rel}}$.

The logarithmic flow-referencing scheme provides a very effective way of eliminating the effects of system flowrate and temperature fluctuations during the separation. In this manner, the viscometer output signals assume the relationship

$$S = \ln \Delta P_A - \ln \Delta P_R = \ln(\Delta P_A/\Delta P_R) \quad (3)$$

With typical solvent flow rate and viscosity conditions used in TFFF (and in viscometric measurements), the detected pressure drop (ΔP) across the capillary is expected to behave according to the Poiseuille's viscosity law for laminar flow:

$$\Delta P = GkQ\eta \quad (4)$$

where G is the electronic gain, k is the capillary geometrical constant, Q is the volume flow rate, η is the viscosity of the flowing liquid, and

$$k = 8L/\pi R^4 \quad (5)$$

where L is the capillary length and R is the internal radius of the capillary. Substituting solvent viscosity η_0 for η in eq. (4) to express the reference ΔP_R , one obtains from eq. (3):

$$S = \ln(G_A k_A Q_A \eta / G_R k_R Q_R \eta_0) \quad (6)$$

where the subscripts A and R refer to the analytical and reference capillaries, respectively. Since $Q_A = Q_R$ for capillaries connected in series, flow rate effects cancel to give

$$S = \ln(G_A k_A \eta / G_R k_R \eta_0) = \ln(\eta/\eta_0) + \ln(G_A k_A / G_R k_R) \quad (7)$$

The second term in eq. (7) is a zero offset factor for the TFFF solvent that forms the viscosity detector baseline S_0 . At $\eta = \eta_0$, one obtains

$$S_0 = \ln(\eta/\eta_0) + \ln(G_A k_A / G_R k_R) = \ln(G_A k_A / G_R k_R) \quad (8)$$

Therefore, the TFFF viscosity signal in excess of the solvent baseline gives the direct measure of desired quantity of $\ln \eta_{\text{rel}}$:

$$\Delta S = S - S_0 = \ln(\eta/\eta_0) = \ln \eta_{\text{rel}} = \eta_{\text{inh}} \times C \quad (9)$$

and, at high sample dilution,

$$\Delta S = [\eta] \times C \quad (10)$$

Since the sample concentration C of the TFFF effluent also is monitored by the differential refractometer, the polymer $[\eta]$ value at every TFFF elution-volume "slice" can be directly determined by the ratio of the excess viscometer signal ΔS to the refractometer signal C , according to eq. (10). By this means, the $[\eta]$ distribution curves for the polymer samples can be obtained. *The sample $[\eta]$ distribution curves so acquired are absolute, without the need of calibration. Such a $[\eta]$ distribution curve is a fundamental property of the polymer sample. The $[\eta]$ distribution of the sample is not affected by the TFFF experimental conditions.* Similarly, this same $[\eta]$ distribution curve can be obtained by SEC as well. However, differences in separation resolution between SEC and TFFF techniques can produce small differences in the results generated by the two methods.

EXPERIMENTAL

TFFF

Time-delayed exponential-decay temperature programming (TDE-TFFF) was used in the experiments to provide uniform separation resolution across the TFFF elution profile. Equipment for this study has previously been described.⁶⁻⁸ Separations were carried out using the following conditions: channel thickness, 132 μm ; initial hot block temperature, 90°C; cold block temperature (constant), 20°C; time delay, exponential decay constant $\tau = 25.0$ min; mobile phase, dioxane or toluene; flow rate, 0.15 mL/min; sample, 100 μL .

Viscometer

Flow capillaries (Fig. 2) were made of stainless steel tubing, 1/16-in. o.d. and 0.016 in. i.d. \times 4 in. long. A delay volume of 18 mL was used between these capillaries. Pressure transducers (Celesco Transducer Products, Inc., Canoga Park, CA) were of 1 psi rating. A differential log amplifier designed in this laboratory was used.¹¹⁻¹³ The capillaries and transducers were immersed in an open water bath at ambient temperature. Drop-time intrinsic viscosities of individual polystyrene and poly(methyl methacrylate) standards were measured in toluene (30°C) with a Type CUD Ubbelohde glass capillary viscometer (VWR Scientific, San Francisco, CA).

Reagents

Solvents were distilled-in-glass grade (Burdick and Jackson, Muskegon, MI). Polymer standards were from Polymer Laboratories, Inc. (Amherst, MA).

Computer Software

The software developed for this work was written in FORTRAN 77 on a Hewlett Packard 1000 Series computer. Separation data were collected on a Hewlett-Packard LAS data handling system. The TFFF-viscosity software

program accounts for the volume difference between the in-series refractometer and viscometer arrangement. With proper adjustment of the volume offset between the detectors, the corresponding TFFF elution-time "slice" of the refractometer and viscometer outputs can be aligned to calculate the $[\eta]$ value at every TFFF retention time.

According to eq. (10), the $[\eta]$ value for the i th TFFF retention time $t_{R,i}$:

$$[\eta]_i = (\Delta S)_i / C_i \quad (11)$$

The following statistical averages of the sample intrinsic viscosity can be calculated:

$$[\eta]_0 = \sum C_i / \sum (C_i / [\eta]_i) \quad (12)$$

$$[\eta]_{+1} = \sum C_i [\eta]_i / \sum C_i \quad (13)$$

$$[\eta]_{+2} = \sum C_i [\eta]_i^2 / \sum C_i [\eta]_i \quad (14)$$

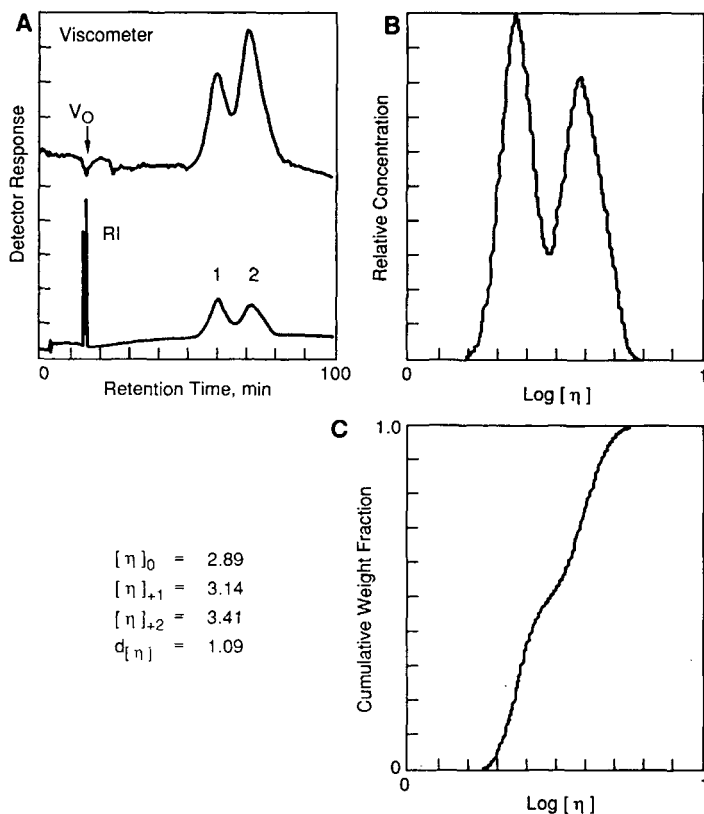


Fig. 3. Intrinsic viscosity-distribution data for two-component polystyrene standards mixture: (A) Fractogram of mixture with refractive index and viscosity detectors. Channel, 132 μm ; mobile phase, toluene; flow rate, 0.15 mL/min; initial hot block temperature, 90°C; cold block temperature (constant), 20°C; time delay, decay constant, τ , 25.0 min; sample: (1) 860,000 and (2) 1,850,000 MW polystyrene standards, 100 μL of 0.125 mg/mL each in toluene. (B) Relative concentration vs. $\log[\eta]$. (C) Cumulative weight fraction vs. $\log[\eta]$.

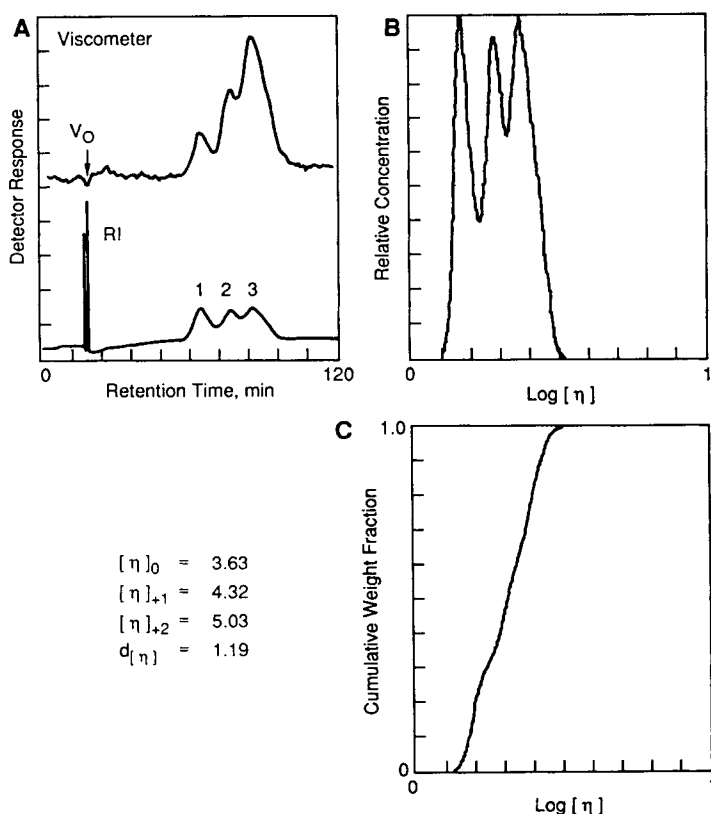


Fig. 4. Intrinsic viscosity–distribution data for three-component polystyrene standards mixture: (A) Fractogram of mixture with refractive index and viscosity detectors. Separation conditions same as in Figure 3, except (1) 860,000, (2) 1,850,000, and (3) 3,600,000 MW polystyrene standards, 100 μL of 0.125 mg/mL each in toluene. (B) Relative concentration vs. $\log[\eta]$. (C) Cumulative weight fraction vs. $\log[\eta]$.

where $[\eta]_{+1}$ = the bulk intrinsic viscosity (weight-average $[\eta]$) of the polymer sample. The ratios between the statistical averages give a measure of sample polydispersity (i.e., the larger the ratios, the broader the polymer MWD).

RESULTS AND DISCUSSION

The results in Figure 3(A) show the TFFF elution profile of a sample mixture of two polystyrene (PS) standards as detected by the viscometer (top curve) and the refractometer (bottom curve). The late-eluting peaks in TFFF fractogram correspond to the higher MW components of the sample; these give the higher viscosity responses, as evident in the results. Figure 3 also gives the $[\eta]$ -distribution summary for this sample. Figure 3(B) shows the differential $[\eta]$ -distribution curve; Figure 3(C) the cumulative $[\eta]$ distribution. The $[\eta]$ -average values reported in dL/g units are also listed at the left of Figure 3. Figure 4 shows similar results for a mixture of three polystyrene standards. Figures 5 and 6 give the results for two sample mixtures of three poly(methyl methacrylate) (PMMA) standards.

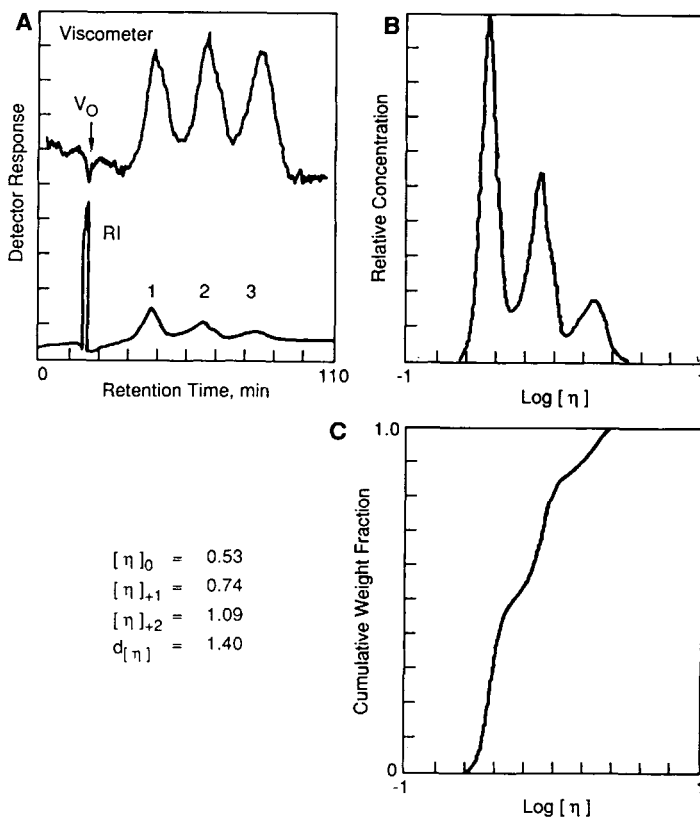


Fig. 5. Intrinsic viscosity-distribution data for three-component poly(methyl methacrylate) standards mixture: (A) Fractogram of mixture with refractive index and viscosity detectors. Separation conditions same as in Figure 3, except (1) 400,000, (2) 840,000, and (3) 1,600,000 MW poly(methyl methacrylate) standards, 100 μ L, 0.5 mg/mL each in toluene. (B) Relative concentration vs. $\log[\eta]$. (C) Cumulative weight fraction vs. $\log[\eta]$.

Drop-time intrinsic viscosity values measured for the individual polymer standards used in this work are given in Table I. Viscosity averages determined for the mixtures by TFFF are tabulated in Table II. The high polydispersity ratios of the test sample mixtures are expected because of the broad-MWD nature of the prepared mixtures. Since the samples in this study were prepared from linear polymer standards, the polydispersity index of the viscosity distribution increases as the mixture molecular-weight distribution increases, as shown in Figure 7. Both polydispersity indices reflect the broadness of the sample molecular weight distribution. A distinct advantage of the viscosity polydispersity value is that this quantity is measured directly without the need for calibration.

Intrinsic viscosity-average values for the mixtures calculated from drop-time viscosity measurements (Table I) are listed in parentheses in Table II for comparison with measured TFFF values. General agreement between online measurements by TFFF and drop-time values is excellent. Close agreement of $[\eta]_{+1}$ values between online and drop-time measurements also was found. It should be noted that $[\eta]_{+1}$ is equivalent to the bulk intrinsic viscosity of the

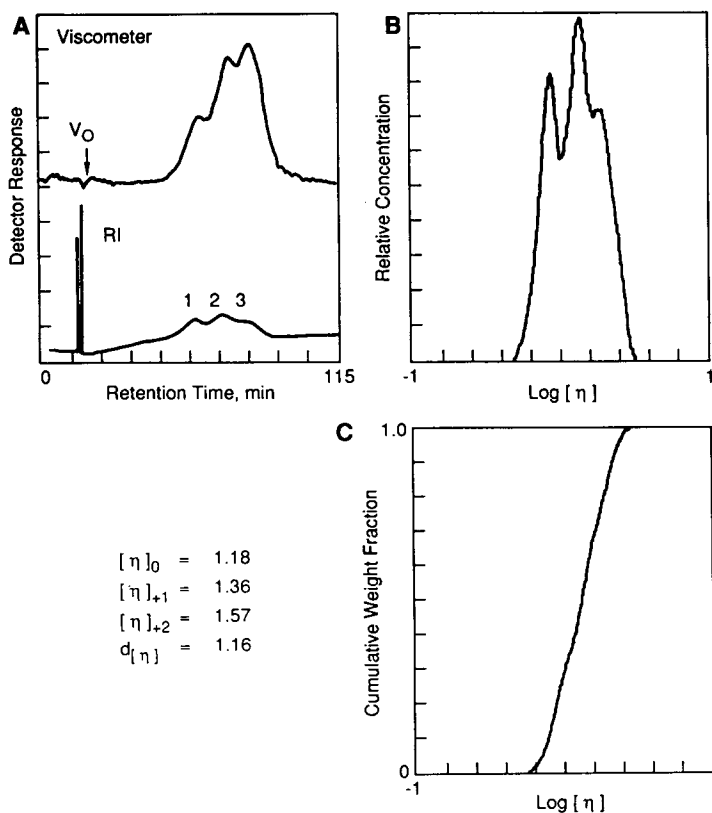


Fig. 6. Intrinsic viscosity-distribution data for another three-component poly(methyl methacrylate) standards mixture: (A) Fractogram of mixture with refractive index and viscosity detectors. Separation conditions same as in Figure 3, except (1) 127,000, (2) 400,000, and (3) 1,600,000 MW poly(methyl methacrylate) standards, 0.75, 0.50, and 0.25 mg/mL, respectively. (B) Relative concentration vs. $\log[\eta]$. (C) Cumulative weight fraction vs. $\log[\eta]$.

TABLE I
Drop-Time Intrinsic Viscosities for Narrow Molecular-Weight Distribution Polymer Standards

Standards	Nominal MW ^a	$[\eta]_{\text{toluene, } 30^\circ\text{C}}$ (dL/g)
PS	3,600,000	6.200
	1,850,000	3.967
	860,000	2.194
PMMA	1,600,000	2.122
	840,000	1.363
	400,000	0.865
	127,000	0.384

^aManufacturer's molecular weight value; PS = polystyrene; PMMA = poly(methyl methacrylate).

TABLE II
 TFFF-Viscosity-Average Results for Polymer Mixtures

Sample composition	MW averages $\times 10^{-3}$			d_{MW}^a	[η] Averages (dL/g)			
	\bar{M}_n	\bar{M}_w	\bar{M}_z		[η] ₀	[η] ₊₁	[η] ₊₂	$d_{[\eta]}^a$
PS: 860, 1850K (1:1)	1170	1360	1540	1.15	2.89 (2.83)	3.14 (3.08)	3.41 (3.34)	1.09 (1.09)
PS: 860, 1850, 3600 (1:1:1)	1514	2103	2713	1.39	3.63 (3.45)	4.32 (4.12)	5.03 (4.77)	1.19 (1.19)
PMMA: 400, 840, 1600K (1:1:1)	695	947	1206	1.36	1.18 (1.27)	1.36 (1.45)	1.57 (1.63)	1.16 (1.14)
PMMA: 127, 400, 1600K (3:2:1)	205	464	1053	2.26	0.53 (0.57)	0.74 (0.83)	1.09 (1.29)	1.40 (1.47)

^a Polydispersity ratio, $d_{\text{MW}} = M_w/M_n$; $d_{[\eta]} = [\eta]_{+1}/[\eta]_0$. Values in parentheses for mixtures are calculated from drop-time viscosity measurements.

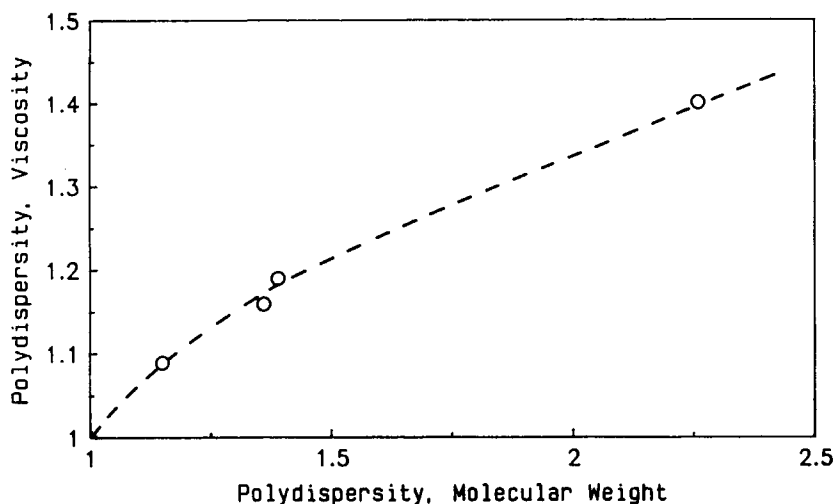


Fig. 7. Correlation of molecular weight with viscosity polydispersity indices.

sample [η]. Since both TFFF/online viscometry and drop-time measurements are subject to finite signal-to-noise limitations, best agreement between the two methods occurs when the overall sample intrinsic viscosity level is relatively high. A more detailed study on the accuracy and precision of TFFF/online viscometry quantitation is planned for a future publication.

[η] and MW Calibration

In SEC, the MW-calibration plots for different polymers converge into a single line when the hydrodynamic volume ($M[\eta]$) is plotted vs. the elution volume.¹⁴ The existence of such a universal calibration plot substantiates the theory that SEC separates by a size-exclusion mechanism, and that an online viscometer enables a true SEC-MW calibration.^{11,12} However, unlike SEC, in

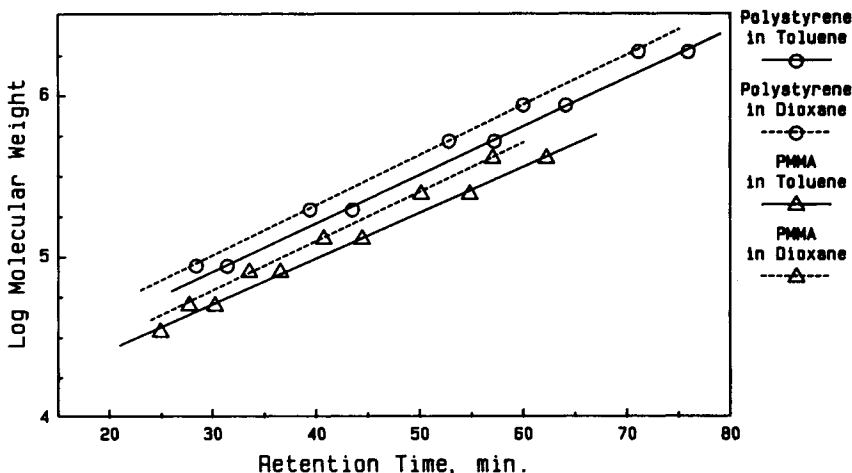


Fig. 8. TDE-TFFF molecular weight calibration plots. Conditions same as in Figure 3, except toluene and dioxane mobile phases; refractive index detector only: PS in toluene; (—○—); (---○---) PS in dioxane; (—△—) PMMA in toluene; (---△---) PMMA in dioxane.

TFFF a plot of the product of $[\eta]$ and molecular weight (M) vs. retention volume does *not* give a universal calibration. Figure 8 shows the log MW vs. retention plots produced by TDE-TFFF for polystyrene and PMMA standards in two different solvents, toluene and dioxane. As noted in other studies, the slopes of these calibration plots typically are very similar, but different intercepts are found for different polymers in different solvents.¹⁵ The $\log[\eta]$ vs. retention time calibration plots for these systems are shown in Figure 9; no common calibration plot is obtained. Figure 10 also shows that the $\log([\eta]MW)$ vs. retention time plot of these calibration data does not give a TFFF universal calibration plot.

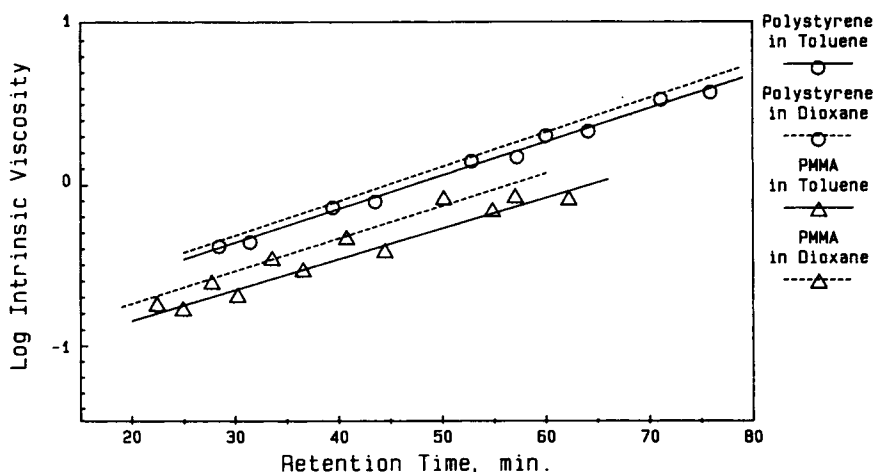


Fig. 9. TDE-TFFF viscosity calibration plots. Conditions same as in Figure 8; viscosity of standards measured offline with capillary viscometer.¹¹: (—○—) PS in toluene; (---○---) PS in dioxane; (—△—) PMMA in toluene; (---△---) PMMA in dioxane.

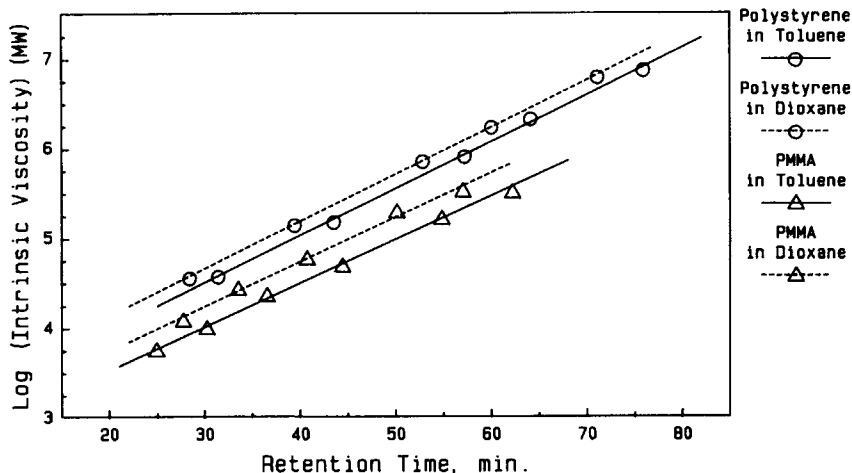


Fig. 10. TDE-TFFF intrinsic viscosity-molecular weight calibration plots. Conditions same as in Figures 8 and 9: (—○—) PS in toluene; (---○---) PS in dioxane; (—△—) PMMA in toluene; (---△---) PMMA in dioxane.

The results of Figures 8–10 have two practical implications. First, these results prove that TFFF retention is not strictly based on the molecular size. Second, when used with TFFF, the viscometer can give $[\eta]$ information on the sample, but not the TFFF-MW calibration curve. Nevertheless, we believe that $[\eta]$ distribution of samples measured by an on-line viscometer with TFFF is a valuable new method for polymer characterization. The approach is especially useful for characterizing ultrahigh MW polymers at low shear rates for which the TFFF technique is especially suited.

The intrinsic viscosity distribution curves and the various viscosity average values (Figs. 3–6) are unique features of individual samples. Such results are expected to be independent of polymer fractionation methods and the experimental conditions used in the analyses. A study of the invariance of sample intrinsic viscosity distributions obtained in this manner is underway.

We thank G. A. Smith and V. E. Burton for performing many of the TFFF and online viscometry experiments. We also thank P. A. Ware and M. C. Han for determining drop-time viscosities for the polymer standards.

References

1. M. N. Myers, K. D. Caldwell, and J. C. Giddings, *Sep. Sci.*, **9**, 47 (1974).
2. J. C. Giddings, M. Martin, and M. N. Myers, *J. Chromatogr.*, **158**, 419 (1978).
3. J. C. Giddings, M. N. Myers, and J. Janca, *J. Chromatogr.*, **186**, 37 (1979).
4. M. Martin and R. Reynaud, *Anal. Chem.*, **52**, 2293 (1980).
5. J. Janca and K. Kleparnik, *Sep. Sci. Technol.*, **16**, 657 (1981).
6. J. J. Kirkland and W. W. Yau, *Macromol.*, **18**, 2305 (1985).
7. J. J. Kirkland and W. W. Yau, *J. Chromatogr.*, **353**, 95 (1986).
8. J. J. Kirkland, S. W. Rementer, and W. W. Yau, *Anal. Chem.*, **60**, 610 (1988).

9. G. H. Thompson, M. N. Myers, and J. C. Giddings, *Anal. Chem.*, **41**, 1219 (1969).
10. M. E. Hovingh, G. H. Thompson, and J. C. Giddings, *Anal. Chem.*, **42**, 195 (1970).
11. W. W. Yau, G. A. Smith, and M. Y. Keating, in *ACS Symp. Ser. 352*, T. Provder, Ed., American Chemical Society, Washington, DC, 1987, p. 80.
12. W. W. Yau and S. W. Rementer, *International GPC Proceedings*, Millipore Corp., Milford, MA, 1987, p. 148.
13. S. D. Abbott and W. W. Yau, U.S. Pats. 4,578,990 and 4,627,271 (1986).
14. H. Benoit, P. Rempp, and Z. Grubisic, *J. Polym. Sci.*, **B5**, 753 (1967).
15. J. J. Kirkland, L. S. Boone, and W. W. Yau, to appear.

Received July 19, 1988

Accepted September 23, 1988